Available online at www.sciencedirect.com
SCIENCE DIRECT®
Journal of Solid State Chemistry 179 (2006) 2020–2026
JOURNAL OF SOLID STATE CHEMISTRY
www.elsevier.com/locate/jssc

Preparation and properties of amorphous titania-coated zinc oxide nanoparticles

Min-Hung Liao[a,*], Chih-Hsiung Hsu[b], Dong-Hwang Chen[b]

[a]*Applied Science and Technology Research Center, Department of Cosmetology and Styling, Transworld Institute of Technology, Douliu 640, Yulin, Taiwan*
[b]*Department of Chemical Engineering, National Cheng Kung University, Tainan, Taiwan 701, ROC*

Received 23 January 2006; received in revised form 24 March 2006; accepted 25 March 2006
Available online 1 April 2006

Abstract

Amorphous TiO_2-coated ZnO nanoparticles were prepared by the solvothermal synthesis of ZnO nanoparticles in ethanol and the followed by sol–gel coating of TiO_2 nanolayer. The analyses of X-ray diffraction (XRD) and transmission electron microscopy (TEM) revealed that the resultant ZnO nanoparticles were hexagonal with a wurtzite structure and a mean diameter of about 60 nm. Also, after TiO_2 coating, the TEM images clearly indicated the darker ZnO nanoparticles being surrounded by the lighter amorphous TiO_2 layers. The zeta potential analysis revealed the pH dependence of zeta potentials for ZnO nanoparticles shifted completely to that for TiO_2 nanoparticles after TiO_2 coating, confirming the formation of core-shell structure and suggesting the coating of TiO_2 was achieved via the adhesion of the hydrolyzed species $Ti–O^-$ to the positively charged surface of ZnO nanoparticles. Furthermore, the analyses of Fourier transform infrared (FTIR) and Raman spectra were also conducted to confirm that amorphous TiO_2 were indeed coated on the surface of ZnO nanoparticles. In addition, the analyses of ultraviolet–visible (UV–VIS) and photoluminescence (PL) spectra revealed that the absorbance of amorphous TiO_2-coated ZnO nanoparticles at 375 nm gradually decreased with an increase in the Ti/Zn molar ratio and the time for TiO_2 coating, and the emission intensity of ZnO cores could be significantly enhanced by the amorphous TiO_2 shell.

Keywords: ZnO; TiO_2; Core-shell; Nanoparticles; Photoluminescence

1. Introduction

Semiconductor nanoparticles have been the subject of great interest due to their size-tunable physical properties and potential applications in diverse areas such as biomedicine, luminescence, photocatalysis, solar cells, display panels, single-electron transistors, and so on [1]. Over the past few years, the surface passivation of semiconductor nanoparticles with a layer of inorganic, organic, or bioactive materials to form the core-shell nanoparticles has attracted considerable attention [2]. The concept of geometric design usually relates to the applied areas [3]. For the use of semiconductor nanoparticles as luminescent materials, their surface properties significantly affect the optical properties because their surface states are known for their photodegradation and luminescent quenching sites. The surface states are likely to trap electrons and/or holes and induce the non-radiative recombination of these charge carriers, leading to the reduction of luminescence efficiency. Recently, the concept of quantum confinement by the band-gap engineering of the heterostructured semiconductor nanoparticles has been suggested to increase the quantum yield or the photoluminescence (PL) intensity [1]. From this viewpoint, many semiconductor nanoparticles capped with the higher band-gap or dielectric insulation materials have been designed and synthesized in recent years such as CdSe on ZnSe [4], CdS on CdSe [5], SiO_2 on CdSe [6], and so on. Additionally, the coating of organic dye molecules on the semiconductor nanoparticles has potential use in solar cells [7]. Therefore, the core-shell nanoparticles based on the semiconductor nanoparticles have clearly scientific meanings including enhanced PL,

*Corresponding author. Fax: +886 6 2092437.
E-mail addresses: liaomh@mail.tit.edu.tw (M.-H. Liao), chendh@mail.ncku.edu.tw (D.-H. Chen).

0022-4596/$ - see front matter © 2006 Elsevier Inc. All rights reserved.
doi:10.1016/j.jssc.2006.03.042

improved stability against photochemical oxidation, enhanced processability, and engineered band structures in the developing nanotechnology [8].

Among the semiconductor nanoparticles, ZnO nanoparticles attract our attention due to their potential applications in photocatalyst and UV laser [9,10]. ZnO is a candidate for UV lasing materials, but its UV emission is not enough for practicability [11,12]. Therefore, several researchers embedded ZnO nanoparticles in the higher band-gap or dielectric insulation matrixes to improve the emission intensity, such as SiO_2 [12], MgO [13], CaF_2 [14], BN [15], and polymer [16]. Additionally, as a photocatalyst, ZnO nanoparticles could not be utilized in the acid solutions [17]. So, their reputation in photocatalysis is not as well as titania. According to the above, the surface modification of ZnO nanoparticles is necessary for their practical applications.

In this work, ZnO nanoparticles were coated with the amorphous TiO_2 nanolayers. This can meet the above-troublesome problems because TiO_2 has a higher dielectric constant and good tolerance to acid media [18]. To our best knowledge, such core-shell nanoparticles of 1–100 nm have not been reported until now. ZnO nanoparticles were synthesized via a simple and processable solvothermal method. Amorphous TiO_2 nanolayers were coated on the surface of ZnO nanoparticles by sol–gel method. The size, morphology, composition, and structure of final products were characterized by transmission electron microscopy (TEM), energy-dispersive X-ray (EDX) analysis, and X-ray diffraction (XRD). Their surface charges, surface function groups, and surface state were investigated by the analyses of zeta potentials and Fourier transform infrared (FTIR) and Raman spectra. In addition, their optical properties were examined by the measurements of UV–VIS) absorption and PL spectra.

2. Materials and methods

Zinc acetate, 2-hydrate was purchased from J.T. Baker (Phillipsburg). Tetrabutylorthotitanat (TBOT) is the guaranteed reagent of E. Merck (Darmstadt). The reagent-grade water used throughout this work was produced by Milli-Q SP ultra-pure water purification system of Nihon Millipore Ltd., Tokyo. All other chemicals are the guaranteed or analytic-grade reagents commercially available and used without further purification.

ZnO nanoparticles were prepared according to the solvothermal process developed by Du et al. [19]. Typically, 2.5 g of zinc acetate was added into 25 mL of absolute ethanol and then sonicated for 30 min. Then, the mixture was transferred into a teflon-lined autoclave of 100 mL and thermostated in an oven at 180 °C for 24 h. Finally, the white product was collected and washed with absolute ethanol two times and dried in a vacuum oven.

ZnO nanoparticles were coated with amorphous TiO_2 via a sol–gel process. In general, 80 mg of the as-prepared ZnO nanoparticles were first added into a mixture of 9 mL ammonium hydroxide (28%) and 80 mL absolute ethanol, and then sonicated for 1 h (denoted as solution I). Secondly, an appropriate amount of TBOT was added into 7.5 mL of deionized water and then sonicated for 5–10 min (denoted as solution II). Solution II was gradually added into solution I drop by drop (2 mL/min) under vigorous stirring at room temperature. After 4 or 24 h, the precipitant was collected by centrifugation and washed with absolute ethanol two times. Finally, the product was stored in absolute ethanol. In addition, pure TiO_2 nanoparticles were prepared following the above procedures with the addition of 0.1 mL TBOT except in the absence of ZnO nanoparticles.

The size and morphology of the resultant nanoparticles were observed by TEM using a JEOL Model JEM-2010 at 200 kV. The sample for TEM analysis was obtained by placing a drop of the particle-dispersed ethanol solution onto a Formvar-covered copper grid and evaporated in air at room temperature. Before withdrawing the sample, the dispersed solution was sonicated for 1 min to obtain a better particle dispersion on the copper grid. XRD measurement was performed on a Rigaku D/max III.V X-ray diffractometer using Cu$K\alpha$ radiation ($\lambda = 0.1542$ nm). The zeta potentials surface charges were measured on a Malvern ZEN2600 Zetasizer Nano Z. FTIR spectra were recorded on a Nicolet Nexus 470 FT-IR spectrometer. Raman spectra were obtained using a Jobin Yvon-LabRam HR micro-Raman system with the 532 nm laser line. The UV–VIS absorption spectra were measured using a Hitachi U-3210 UV–VIS spectrophotometer. The PL spectra were taken on a Hitachi F-4500 fluorescence spectrophotometer. The sample solutions for the analyses of UV–VIS absorption spectra and PL spectra were prepared by dispersing the nanoparticles in ethanol, with a fixed concentration of 1.0 mg/mL based on the weight of ZnO.

3. Results and discussion

Fig. 1 shows the XRD patterns for ZnO, TiO_2-coated ZnO, and TiO_2 nanoparticles. Nine characteristic peaks ($2\theta = 31.77$, 34.42, 36.25, 47.54, 56.60, 62.86, 66.38, 67.96, and 69.10°), marked by their Miller indices ((100), (002), (101), (102), (110), (103), (200), (112), and (201)) were observed in the case of ZnO nanoparticles. This reveals that the resultant nanoparticles are the hexagonal ZnO nanoparticles with a wurtzite structure (JCPDS no. 36-1451). After TiO_2 coating, the XRD pattern had no significant change and no characteristic peaks for TiO_2 crystalline were observed. Because the XRD pattern of the TiO_2 nanoparticles obtained following the procedures for TiO_2 coating, except in the absence of ZnO nanoparticles, also did not show any characteristic peaks for TiO_2 crystalline, it was suggested that the resultant TiO_2 nanoparticles or shells on the surface of ZnO nanoparticles were amorphous.

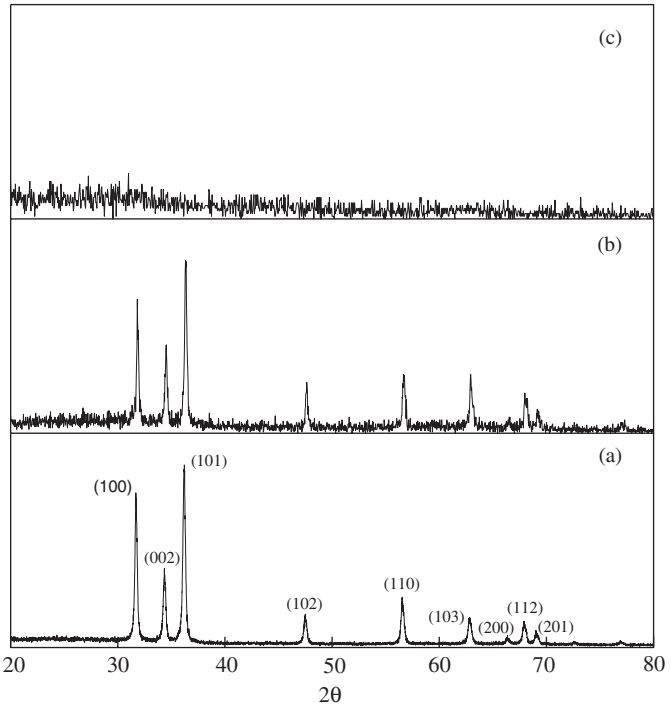

Fig. 1. XRD pattern of ZnO (a), TiO_2-coated ZnO (b), and TiO_2 (c) nanoparticles.

Fig. 2(a) indicates the typical TEM image of ZnO nanoparticles, which revealed the resultant ZnO nanoparticles were discrete essentially with a mean diameter of about 60 nm. Figs. 2(b)–(e) show the typical TEM images of TiO_2-coated ZnO nanoparticles obtained at various Ti/Zn molar ratios and coating times. For both Ti/Zn molar ratios of 0.31 and 0.63, it was observed that the darker ZnO cores were surrounded by the lighter shells. Also, the shell thicknesses at 24 h (~15.1 nm) were significantly thicker than those at 4 h (~5.3 nm). The XRD and EDX analyses indicated the lighter shells were amorphous TiO_2, confirming the formation of core-shell structure and revealing the shell thickness increased with an increase in the time for TiO_2 coating. In addition, the shell thicknesses did not increase significantly with an increase in the Ti/Zn molar ratios. This might be due to the irregular shape and broad size distribution of ZnO nanoparticles as observed in Fig. 2(a). Further clarification was given in the later analyses of UV–VIS absorption and PL spectra.

The zeta potentials of ZnO, TiO_2, and TiO_2-coated ZnO nanoparticles (0.1 mg/mL) in 1.0 mM NaCl at pH 2–11 (adjusted by HCl and NaOH) are shown in Fig. 3. It was obvious that the pH dependence of zeta potentials for ZnO nanoparticles shifted completely to that for TiO_2 nanoparticles after TiO_2 coating, also confirming the formation of core-shell structure. Furthermore, the isoelectric point of ZnO nanoparticles was found to be 9.7, in agreement with the reported value [20] and below which the surface of ZnO nanoparticles was positively charged ($-ZnOH^{2+}$) at pH < 9.7. However, TiO_2 and TiO_2-coated ZnO nanoparticles were negatively charged over the whole pH range examined. In addition, since the solution pH was about 8–9 during the coating of TiO_2, it was suggested that the coating of TiO_2 was achieved via the adhesion of the hydrolyzed species Ti–O^- of TBOT [21] to the positively charged surface of ZnO nanoparticles, as suggested by Zhang and Li [22] in the study of TiO_2 coating on the surface of ZnS nanoparticles.

Fig. 4 shows the FTIR spectra of ZnO, TiO_2, and TiO_2-coated ZnO nanoparticles obtained at a coating time of 24 h and a Ti/Zn molar ratio of 0.31 and 0.63. In the wavenumber range examined, there were no significant characteristic peaks for ZnO nanoparticles. However, for TiO_2 and TiO_2-coated ZnO nanoparticles, five characteristic peaks at 1650, 1400, 1240, 1160, and 1080 cm^{-1} were observed. The peak at 1650 cm^{-1} resulted from the adsorbed H_2O molecules, which were not removed completely after sol–gel synthesis or coating of TiO_2. The peak at 1400 cm^{-1} was attributed to the vibration mode of Ti–O bond [23], and all those at 1240, 1160, and 1080 cm^{-1} should be due to the Ti–OH bond [24]. The comparison of FTIR spectra revealed that TiO_2 was indeed coated on the surface of ZnO nanoparticles.

The Raman spectra of ZnO, TiO_2, and TiO_2-coated ZnO nanoparticles obtained at a Ti/Zn molar ratio of 0.31 and a coating time of 24 h are indicated in Fig. 5. For the ZnO nanoparticles, a significant E_2 mode at 438.5 cm^{-1} was observed [25]. This characteristic peak was the same as that of the bulk ZnO, without significant red shift due to the optical phonon confinement as exhibited by those smaller than 5 nm [25]. This might be attributed to the fact that the ZnO nanoparticles obtained in this work (about 60 nm) were not small enough. For the TiO_2 nanoparticles, two characteristic peaks that appeared at 447 and 612 cm^{-1} could be attributed to the Raman scattering of E_g mode and A_{1g} mode, respectively [26]. For the TiO_2-coated ZnO nanoparticles, it was obvious that the A_{1g} mode of TiO_2 at 612 cm^{-1} significantly shifted to 780 cm^{-1}. Such a large red shift in the wavenumber of Raman scattering might have resulted by the structural change [27]. In this case, TiO_2 was present in the form of a shell instead of a particle.

The UV–VIS absorption spectra of ZnO and TiO_2-coated ZnO nanoparticles obtained at various Ti/Zn molar ratios and coating times are shown in Fig. 6. It was found that the absorbance at the characteristic absorption band of ZnO nanoparticles occurred at 375 nm and decreased significantly after TiO_2 coating. Also, the absorbance decreased with the increase in the Ti/Zn molar ratio and coating time. This revealed the presence of amorphous TiO_2 shells that led to a shielding effect for the absorption of ZnO nanoparticles around 375 nm. In addition, the effect of physically mixing between amorphous titania and ZnO nanoparticles on the UV–VIS absorption spectrum was also investigated. As shown in Fig. 6, the physically mixing of amorphous titania and ZnO nanoparticles did not result in the significant decrease in the absorbance of ZnO nanoparticles around 375 nm. Furthermore, the

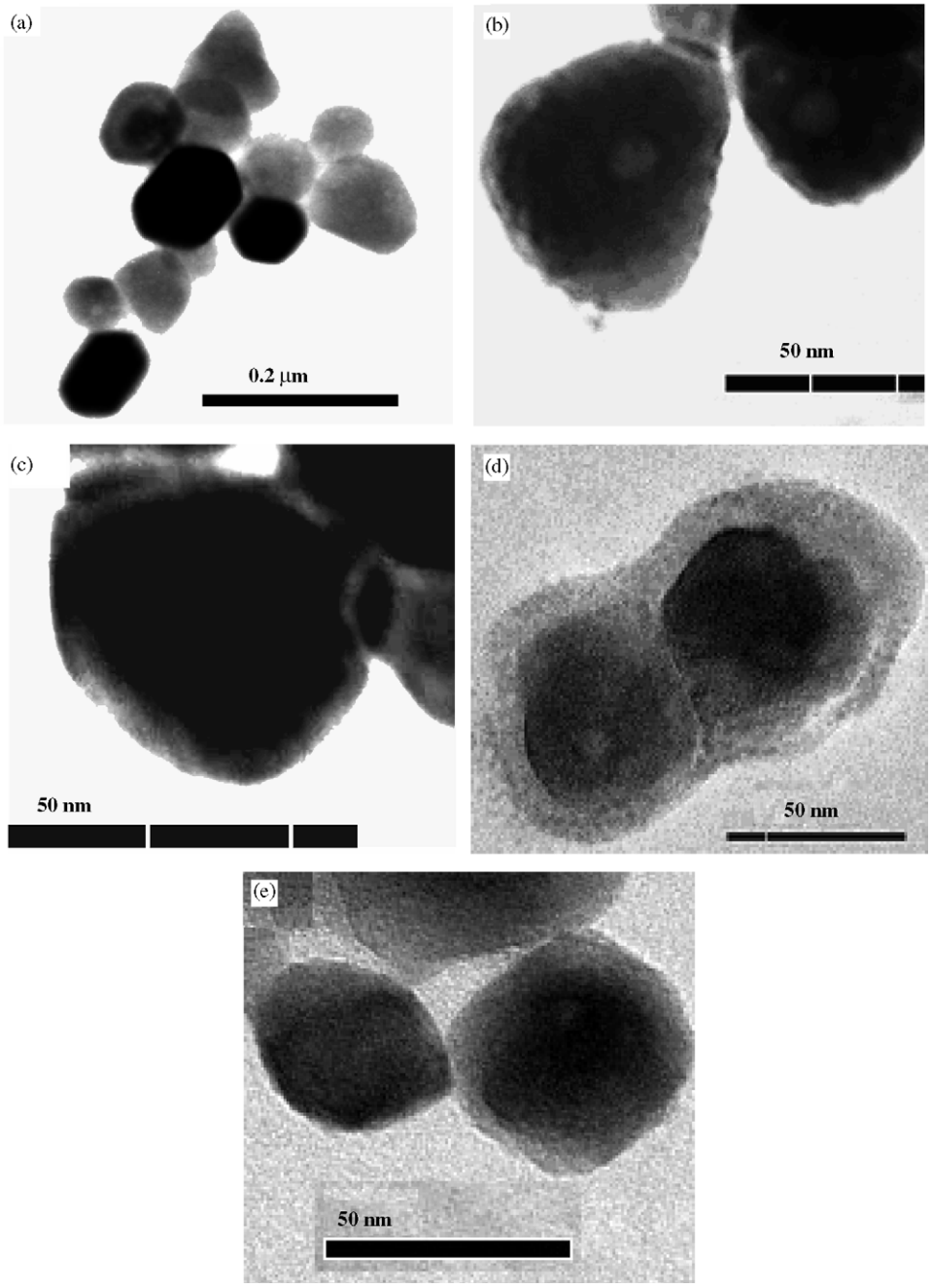

Fig. 2. Typical TEM images of ZnO nanoparticles (a) and TiO_2-coated ZnO nanoparticles obtained at various Ti/Zn molar ratios and coating times; (b) Ti/Zn = 0.31, 4 h; (c) Ti/Zn = 0.63, 4 h; (d) Ti/Zn = 0.31, 24 h; and (e) Ti/Zn = 0.63, 24 h.

sample solutions for the analysis of UV–VIS absorption spectra had a fixed concentration of 1.0 mg/mL based on the weight of ZnO nanoparticles. So, the shielding effect could not be referred to the intermixing between amorphous titania and ZnO nanoparticles or to the variation of Ti/Zn molar ratio. Although the effect of Ti/Zn molar ratio on the thickness of TiO_2 shells could not clearly be observed from the TEM images shown in Fig. 2, the shielding degree suggested that the thickness of TiO_2 shells should increase with an increase in the Ti/Zn molar ratio.

Fig. 7 shows the PL spectra of ZnO and TiO_2-coated ZnO nanoparticles obtained at various Ti/Zn molar ratios and coating times, with an excitation wavelength of 350 nm. For the ZnO nanoparticles, there were a stronger characteristic peak at 380 nm and a weaker characteristic peak around 500 nm, due to the near-band-edge emission and the deep-level emission, respectively [28]. After coated by amorphous TiO_2, the PL intensities at 380 nm were enhanced significantly and the characteristic peaks were slightly blue shifted. The enhancement could be ascribed to the surface passivation of ZnO nanoparticles by the

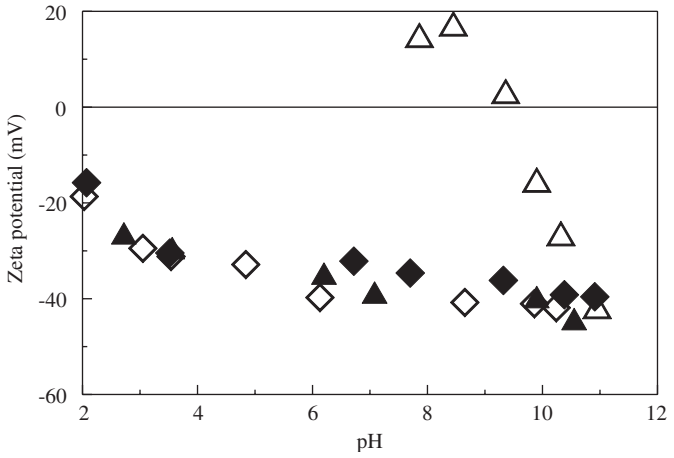

Fig. 3. pH-dependence of zeta potentials for ZnO (△) TiO_2 (◇), and TiO_2-coated ZnO nanoparticles obtained at a coating time of 24 h and a Ti/Zn molar ratio of 0.31 (◆) and 0.63 (▲).

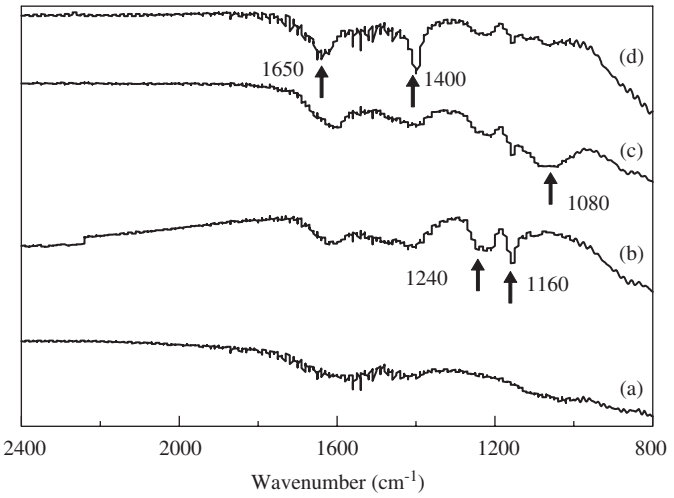

Fig. 4. FTIR spectra of ZnO (a), TiO_2 (d), and TiO_2-coated ZnO nanoparticles obtained at a coating time of 24 h and a Ti/Zn molar ratio of 0.31 (b) and 0.63 (c).

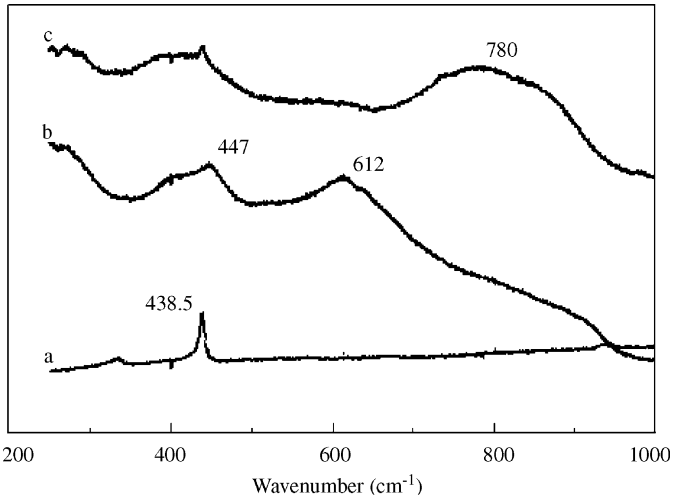

Fig. 5. Raman spectra of ZnO (a), TiO_2 (b), and TiO_2-coated ZnO nanoparticles obtained at a Ti/Zn molar ratio of 0.31 and a coating time of 24 h (c).

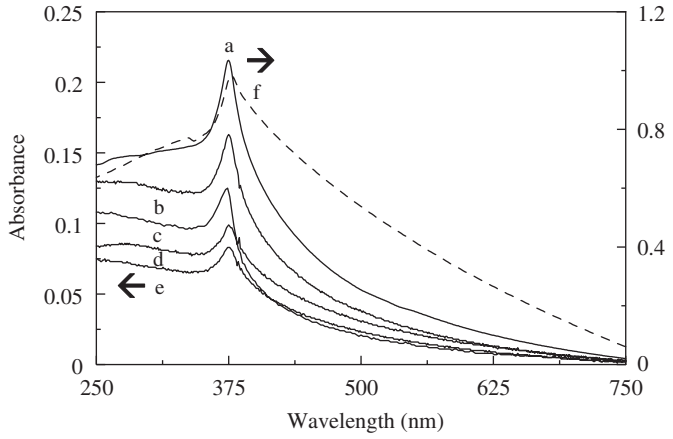

Fig. 6. UV–VIS spectra of ZnO nanoparticles (a), the physical mixing with ZnO nanoparticles and amorphous TiO_2 (f), and TiO_2-coated ZnO nanoparticles obtained at various Ti/Zn molar ratios and coating times: (b) Ti/Zn = 0.31, 4 h; (c) Ti/Zn = 0.63, 4 h; (d) Ti/Zn = 0.31, 24 h; (e) Ti/Zn = 0.63, 24 h.

amorphous TiO_2 shells, which effectively eliminated the dangling bonds or coordination sites on the surface of ZnO nanoparticles. Thus, the photogenerated carriers (electrons and holes) would not be trapped by the dangling bonds or coordination sites. Hence, the electrons and holes could be mostly confined in the inside of ZnO nanoparticles. This nano-confinement effect increased the possibility for the recombination of electrons and holes, and led to the enhancement in PL intensity. As for the slight blue shift of the near-band-edge emission peak, it revealed that the band-gap energies of TiO_2-coated ZnO nanoparticles were larger than that of ZnO nanoparticles (3.3 eV [29,30]), disclosing the possibility of tuning the band-gap energy via surface modification. Additionally, the spectra around 380 nm may consist of several peaks because zinc vacancies in ZnO lattice cause violet emission around 405 nm [30]. The lattice defect might be eliminated by TiO_2 coating and led to the similarly blue shift of PL spectra. This is another possible mechanism for the blue shift. Furthermore, the enhancement decreased slightly with an increase in the Ti/Zn molar ratio and coating time. This might be because thicker TiO_2 shells had a stronger shielding effect for the absorption of excitation energy by ZnO nanoparticles [31].

In addition, although the exact mechanism is still controversial, the deep-level emission is known to originate from singly ionized oxygen vacancies, oxygen interstitial, zinc vacancies, and interface/surface-related defect states [32]. The origin of green emission at 500 nm has been found to be due to the oxygen vacancies as shown by the results of many studies [33]. So, the PL spectra in Fig. 7 revealed a lattice defect condition of TiO_2-coated ZnO nanoparticles. This leads to the mechanism of surface passivation and PL enhancement. In Fig. 7, the coating of amorphous TiO_2 enhanced the PL intensities significantly around 500 nm.

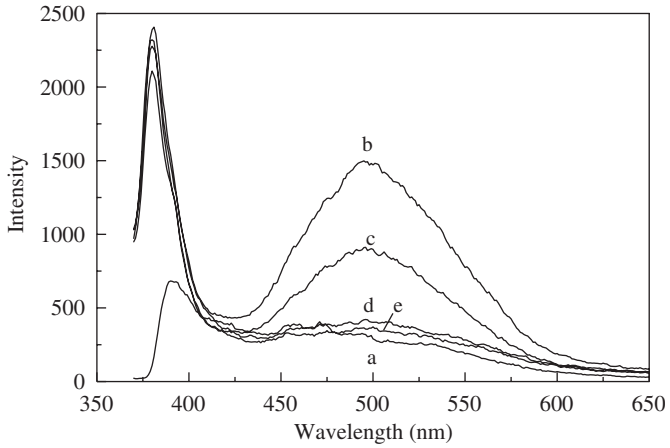

Fig. 7. Photoluminescence spectra of ZnO nanoparticles (a) and TiO_2-coated ZnO nanoparticles obtained at various Ti/Zn molar ratios and coating times: (b) Ti/Zn = 0.31, 4 h; (c) Ti/Zn = 0.63, 4 h; (d) Ti/Zn = 0.31, 24 h; and (e) Ti/Zn = 0.63, 24 h.

However, the enhancement decreased gradually with an increase in the Ti/Zn molar ratio and coating time. This implied that the thin shells of amorphous TiO_2 coated on the surface of ZnO nanoparticles provided many ionized oxygen vacancies, oxygen interstices, and interface/surface-related defects. Furthermore, with an increase in the Ti/Zn molar ratio and coating time, the amorphous TiO_2 shells became thicker and even denser. This might have led to the reduction of ionized oxygen vacancies, oxygen interstices, and interface/surface-related defects, and thereby the enhancement in the deep-level emission around 500 nm became weaker. Thus, the fine control of TiO_2 shell thickness on the surface of ZnO nanoparticles was very important in the enhancement of PL intensity.

4. Conclusions

TiO_2-coated ZnO nanoparticles have been fabricated by the sol–gel coating of TiO_2 on the surface of solvothermal synthesized-ZnO nanoparticles. The analyses of XRD and TEM revealed the ZnO nanoparticles were hexagonal with a wurtzite structure and a mean diameter of about 60 nm, and the TiO_2 shells coated on the surface of ZnO nanoparticles were amorphous. In addition to TEM analysis, the core-shell structure has been confirmed by comparing the zeta potentials, FTIR spectra, and Raman spectra for ZnO and TiO_2-coated ZnO nanoparticles. The analysis of UV–VIS absorption spectra indicated that the absorbance of amorphous TiO_2-coated ZnO nanoparticles at 375 nm gradually decreased with an increase in the Ti/Zn molar ratio and the time for TiO_2 coating, revealing the amorphous TiO_2 shells had a shielding effect for the absorption of ZnO nanoparticles. Also, combining the TEM analysis, it could be concluded that the thickness of TiO_2 shells increased with an increase in the Ti/Zn molar ratio and coating time. The analysis of PL spectra indicated the near-band-edge emission of ZnO nanoparticles at 380 nm was blue shifted and enhanced by the coating of amorphous TiO_2 shells due to the modification of surface property and the increased confinement of photogenerated carriers. The deep-level emission around 500 nm was also significantly enhanced, probably due to the amorphous TiO_2 shells that provided more ionized oxygen vacancies, oxygen interstices, and interface/surface-related defects. However, it was also notable that an increase in the Ti/Zn molar ratio and time for TiO_2 coating led to the decrease in the enhancement of PL intensities, revealing the importance of finely controlling the TiO_2 shell thickness.

Acknowledgments

This work was performed under the auspices of the National Science Council of the Republic of China, under Contract no. NSC93-2214-E-265-002, to which the authors wish to express their thanks.

References

[1] S. Kim, B. Fisher, H.J. Eisler, M. Bawendi, J. Am. Chem. Soc. 125 (2003) 11466–11467.
[2] F. Caruso, Adv. Mater. 13 (2001) 11–22.
[3] C.J. Zhong, M.M. Maye, Adv. Mater. 13 (2001) 1507–1511.
[4] X. Zhong, R. Xie, Y. Zhang, T. Basché, W. Knoll, Chem. Mater. 17 (2005) 4038–4042.
[5] D. Pan, Q. Wang, S. Jiang, X. Ji, L. An, Adv. Mater. 17 (2005) 176–179.
[6] X. Zhou, Y. Kobayashi, V. Romanyuk, N. Ochuchi, M. Takeda, S. Tsunekawa, A. Kasuya, Appl. Surf. Sci. 242 (2005) 281–286.
[7] D.B. Menzies, L. Bourgeois, Y.B. Cheng, G.P. Simon, N. Brack, L. Spiccia, Surf. Coat. Technol. 198 (2005) 118–122.
[8] H. Kim, M. Achermann, L.P. Balet, J.A. Hollingsworth, V.I. Klimov, J. Am. Chem. Soc. 127 (2005) 544–546.
[9] Q. Wan, T.H. Wang, J.C. Zhao, Appl. Phys. Lett. 87 (2005) 083105-1-083105-3.
[10] B. Lin, Z. Fu, Y. Jia, G. Liao, J. Electrochem. Soc. 148 (2001) G110–G113.
[11] E.S.P. Leong, M.K. Chong, S.F. Yu, K. Pita, IEEE Photon. Technol. Lett. 16 (2004) 2418–2420.
[12] Z. Fu, B. Yang, L. Li, W. Dong, C. Jia, W. Wu, J. Phys.: Condens. Matter 15 (2003) 2867–2873.
[13] J.G. Ma, Y.C. Liu, C.L. Shao, J.Y. Zhang, Y.M. Lu, D.Z. Shen, X.W. Fan, Phys. Rev. B 71 (2005) 125430-1-125430-6.
[14] Y.C. Liu, H.Y. Xu, R. Mu, D.O. Henderson, Y.M. Lu, J.Y. Zhang, D.Z. Shen, X.W. Fan, C.W. White, Appl. Phys. Lett. 83 (2003) 1210–1212.
[15] J.F. Li, L.Z. Yao, C.H. Ye, C.M. Mo, W.L. Cai, Y. Zhang, L.D. Zhang, J. Cryst. Growth 223 (2001) 535–538.
[16] L. Guo, S. Yang, C. Yang, P. Yu, J. Wang, W. Ge, G.K.L. Wong, Chem. Mater. 12 (2000) 2268–2274.
[17] A.A. Khodja, T. Sehili, J.F. Pilichowski, P. Boule, J. Photochem. Photobiol. A 141 (2001) 231–239.
[18] S.K. Kim, W.D. Kim, K.M. Kim, C.S. Hwang, J. Jeong, Appl. Phys. Lett. 85 (2004) 4112–4114.
[19] H. Du, F. Yuan, S. Huang, J. Li, Y. Zhu, Chem. Lett. 33 (2004) 770–771.
[20] S. Music, D. Dragcevic, M. Maljkovic, S. Popovic, Mater. Chem. Phys. 77 (2002) 521–530.
[21] F. Zhang, J. Chen, X. Zhang, W. Gao, R. Jin, N. Guan, Catal. Today 93–95 (2004) 645–650.
[22] Y. Zhang, Y. Li, J. Phys. Chem. B 108 (2004) 17805–17811.

[23] X.T. Wang, S.H. Zhong, X.F. Xiao, J. Mol. Catal. A: Chem. 229 (2005) 87–93.
[24] Y. Xie, X. Liu, A. Huang, C. Ding, P.K. Chu, Biomaterials 26 (2005) 6129–6135.
[25] R.D. Yang, S. Tripathy, Y. Li, H.J. Sue, Chem. Phys. Lett. 411 (2005) 150–154.
[26] H. Zhang, X. Luo, J. Xu, B. Xiang, D. Yu, J. Phys. Chem. B 108 (2004) 14866–14869.
[27] C.C. Chen, R.S. Chen, T.Y. Tsai, Y.S. Huang, D.S. Tsai, K.K. Tiong, J. Phys.: Condens. Matter 16 (2004) 8475–8484.
[28] X.D. Gao, X.M. Li, W.D. Yu, Mater. Res. Bull. 40 (2005) 1104–1111.
[29] H.G. Chen, J.L. Shi, H.R. Chen, J.N. Yan, Y.S. Li, Z.L. Hua, Y. Yang, D.S. Yan, Opt. Mater. 25 (2004) 79–84.
[30] S. Zhao, Y. Zhou, K. Zhao, Z. Liu, P. Han, S. Wang, W. Xiang, Z. Chen, H. Lu, B. Cheng, G. Yang, Physica B 373 (2006) 154–156.
[31] H. Li, D. Wang, H. Chen, B. Liu, L. Gao, Macromol. Biosci. 3 (2003) 351–353.
[32] S.J. Chen, Y.C. Liu, C.L. Shao, Y.M. Lu, J.Y. Zhang, D.Z. Shen, X.W. Fan, Chem. Phys. Lett. 397 (2004) 360–363.
[33] F.H. Leiter, H.R. Alves, A. Hofstaetter, D.M. Hofmann, B.K. Meyer, Phys. Stat. Sol. 226 (2001) R4–R5.